Princeton Plasma Physics Laboratory

PPPL-5147

Searching for Enhanced RF Field Amplitudes in the SOL Using a Simplified Cold-Plasma Model

R.J. Perkins, J. C. Hosea, N. Bertelli, E.F. Jaeger,
C. K. Phillips, G. Taylor, J. R. Wilson

July 2015

Prepared for the U.S. Department of Energy under Contract DE-AC02-09CH11466.

Princeton Plasma Physics Laboratory
Report Disclaimers

Full Legal Disclaimer

This report was prepared as an account of work sponsored by an agency of the United States Government. Neither the United States Government nor any agency thereof, nor any of their employees, nor any of their contractors, subcontractors or their employees, makes any warranty, express or implied, or assumes any legal liability or responsibility for the accuracy, completeness, or any third party's use or the results of such use of any information, apparatus, product, or process disclosed, or represents that its use would not infringe privately owned rights. Reference herein to any specific commercial product, process, or service by trade name, trademark, manufacturer, or otherwise, does not necessarily constitute or imply its endorsement, recommendation, or favoring by the United States Government or any agency thereof or its contractors or subcontractors. The views and opinions of authors expressed herein do not necessarily state or reflect those of the United States Government or any agency thereof.

Trademark Disclaimer

Reference herein to any specific commercial product, process, or service by trade name, trademark, manufacturer, or otherwise, does not necessarily constitute or imply its endorsement, recommendation, or favoring by the United States Government or any agency thereof or its contractors or subcontractors.

PPPL Report Availability

Princeton Plasma Physics Laboratory:

http://www.pppl.gov/techreports.cfm

Office of Scientific and Technical Information (OSTI):

http://www.osti.gov/scitech/

Related Links:

U.S. Department of Energy

U.S. Department of Energy Office of Science

U.S. Department of Energy Office of Fusion Energy Sciences

Searching for Enhanced RF Field Amplitudes in the SOL Using a Simplified Cold-Plasma Model

R.J. Perkins[1], J. C. Hosea[1], N. Bertelli[1], E.F. Jaeger[2], C. K. Phillips[1], G. Taylor[1], J. R. Wilson[1]

[1] *Princeton Plasma Physics Laboratory, Princeton, United States*

[2] *XCEL Engineering Inc., Oak Ridge, United States*

NSTX uses a high-harmonic fast-wave (HHFW) antenna for plasma heating and current drive, but a significant amount of the HHFW can be lost along open magnetic fields lines in the SOL to the divertor regions under certain conditions [1,2]. The underlying cause is related to fast-wave propagation in the scrape-off layer (SOL), as the heating efficiency is strongly correlated with the location of the righthand cutoff. Recent results with the full-wave simulation AORSA suggest that the RF electric field amplitude grows to large values in the SOL when the SOL density is large enough that there is no cutoff region in front of the antenna [3]. However, interpretation of the AORSA results have not been straightforward due to the complicated vessel and magnetic geometry [4]. In this paper, we employ a cylindrical cold-plasma model to determine which features of the AORSA results can be reproduced in this simplified geometry. We do indeed find modes that conduct a significant fraction of power in a low density periphery plasma surrounding the dense core plasma, but more work is needed to quantitatively link these results to those from experiments and from AORSA.

The cylindrical cold-plasma model, based on previous work [5], consists of a cylindrical core plasma of radius r_c and density n_c surrounded by a lower-density annulus of radius r_a and density n_a, which is in turn surrounded by a vacuum region with a perfectly conducting vessel of radius r_w. A uniform axial magnetic field is used, which would correspond to a "zero-pitch" tokamak. For each azimuthal wavenumber m, the system dispersion (the system of equations obtained by matching solutions in each region to boundary conditions) is solved for a set of discrete radial modes, denoted by the index n. Each mode has a single axial wavenumber $k_{||}$ and three corresponding radial wavenumbers $k_\perp$, one for each region. In the core and annulus, $k_\perp$ is given by the local cold-plasma dispersion, and while both slow

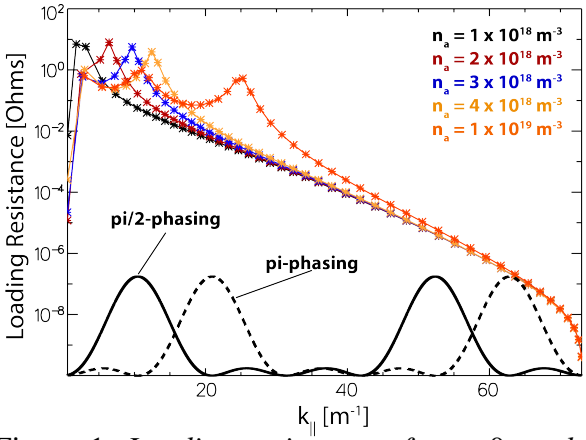

Figure 1: *Loading resistance of $m = 0$ modes peaks at a $k_{||}$ that depends on n_a. Plotted for reference are antenna spectra for $\pi/2$ and π phasing.*

and fast waves are included in the model, in this paper $k_\perp$ will denote the fast-wave branch, the slow wave always being cutoff and confined to a very narrow radial region at the core-annulus and annulus-vacuum interface. In the vacuum region, the modes are always cutoff, with $k_\perp^{\rm vac} = (k_\parallel^2 - \omega^2/c^2)^{1/2} \approx k_\parallel$. We typically model the antenna using four current straps situated at $r = r_s$ with arbitrary phasing, an inter-strap distance 0.15 m, and uniform azimuthal current distribution over an angle of $\pi/2$. A Faraday screen at $r = r_F$ shorts out the E_z-mode from the antenna. We chose parameters to mimic the conditions in NSTX: $n_c = 5\times10^{19}$ m^{-3}, $f = 30$ MHz, $B = 0.323$ T which gives $\omega/\omega_{ci} = 12$, $r_c = 0.515$ m, $r_a = 0.575$ m, $r_F = 0.600$ m, $r_s = 0.650$ m, and $r_w = 0.700$ m.

We begin by analyzing azimuthally symmetric modes ($m = 0$). The loading resistance for each $m = 0$ mode is plotted against the mode axial wavenumber in Fig. 1 for different annulus densities. Loading resistance $R_{m,n}$ is related to the wave power $P_{m,n}$ conducted by each mode via $R_{m,n}I_{\rm ant}^2/2 = P_{m,n}$, with $I_{\rm ant}$ the current in the antenna strap. $P_{m,n}$ is calculated either via the power output of the antenna

$$P_{m,n} = \int \langle \mathbf{E}_{m,n} \cdot \mathbf{J}_{\rm ant} \rangle \, dV, \qquad (1)$$

or via the axial Poynting flux integrated over the cross-section of the cylinder

$$P_{m,n} = \int_{r=0}^{r=r_w} \int_{\theta=0}^{\theta=2\pi} \langle \mathbf{E}_{m,n} \times \mathbf{H}_{m,n} \rangle \, dr d\theta, \qquad (2)$$

where $< \ldots >$ denotes time-averaging of complex quantities. Both methods for computing the mode power give the same result. The mode powers are computed for a single-strap antenna, which uniformly excites all $k_\parallel$, to get a sense of the mode structure without complication from the particular choice of an antenna spectrum. For reference, the spectral shapes for $\pi/2$ and π phasing of a four-strap antenna are plotted in Fig. (1). In general, loading resistance decreases with $k_\parallel$, as the wave fields become more evanescent in the vacuum region with a cutoff wavenumber $k_\perp^{\rm vac} \approx k_\parallel$. However, a peak in loading resistance is clearly seen, and the $k_\parallel$ of the peak increases with the annulus density. The peak always occurs at a $k_\parallel$ lower than the righthand cutoff $c^2k_\parallel^2/\omega^2 = R$.

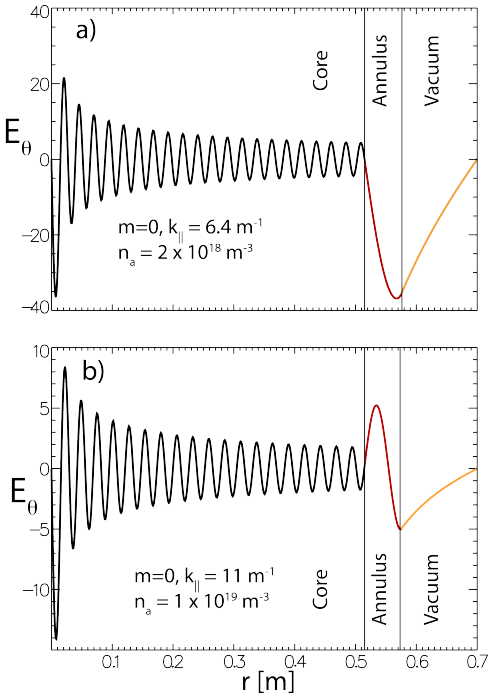

Figure 2: *$E_\theta(r)$ for peak modes is large in the annulus and has an approximate 1/4 or 3/4 wavelength structure there.*

Figure 2a shows the radial profile of E_θ for the peak $m = 0$ mode for $n_a = 2.0\times10^{18}$ m^{-3} (e.g. peak of red curve in Fig. (1)). At the core-annulus interface, $E_\theta \approx 0$, and there is approximately

one quarter wavelength in the annulus region. In the annulus, E_θ is a linear combination of $J_1(k_\perp r)$ and $Y_1(k_\perp r)$; since $k_\perp = 29.2$ m^{-1} in the annulus for this mode, the Bessel functions are well-approximated by their asymptotic forms $\sin(k_\perp r - 3\pi/4)/(k_\perp r)^{1/2}$ and $\cos(k_\perp r - 3\pi/4)/(k_\perp r)^{1/2}$, so we can compute the phase difference across the annulus as $k_\perp(r_a - r_c) = 1.754$, which is indeed just above the quarter-wavelength value of $\pi/2 = 1.571$. Table 1 shows the values of $k_\parallel$, $k_\perp$, and $k_\perp(r_a - r_c)$ for each peak in Fig. 1. While $k_\parallel$ increases markedly with density, $k_\perp$ remains relatively constant. Finally, note that fitting three quarter wavelengths into the annulus would require $k_\perp \approx 79$ m^{-1}, which is above the maximum value that $k_\perp$ can attain for typical SOL densities on NSTX. However, if we raise the annulus density to very large values, we do indeed observe multiple peaks; at $n_a = 1\times10^{19}$ m^{-3} (Fig. 1), the peak mode at $k_\parallel = 11$ m^{-1} has $k_\perp = 78.5$ m^{-1} and a radial E_θ profile given by Fig. 2b.

Table 1: Wavenumbers for peak mode as annulus density increases.

n_a[m^{-3}]	$k_\parallel$ [m^{-1}]	$k_\perp$ [m^{-1}]	$k_\perp(r_a - r_c)$
1×10^{18}	1.80	33.1	1.99
2×10^{18}	6.43	29.2	1.75
3×10^{18}	9.68	29.8	1.99
4×10^{18}	12.4	30.7	1.84
1×10^{19}	25.3	33.5	2.01
1×10^{19}	11.0	78.5	4.71

For a mode to be relevant to the SOL-loss studies on NSTX, it should conduct a significant fraction of the wave power through the annulus. Figure 3 partitions the wave power $P_{m,n}$ (evaluated for unit antenna current) carried by each $m = 0$ mode with $n_a = 2\times10^{18}$ m^{-3} (red curve of Fig. (1)) into power conducted in the core, annulus, and vacuum region by integrating the axial Poynting flux over the appropriate cross-section. Most modes conduct the majority of their power in the core, but the peak mode carries 54% of its power in the annulus, with the average Poynting flux there being four times larger than in the core. Further, this mode accounts for 58% of the total wave power, making such modes relevant to the NSTX studies in that they conduct a significant fraction of the total power through the annulus. Since the antenna spectrum favorably weights modes with $k_\parallel$ that closely match the antenna, one can conceivably explain the SOL loss on NSTX by selecting SOL parameters such that these peak modes which conduct significant power in the annulus lie under the antenna spectrum peak.

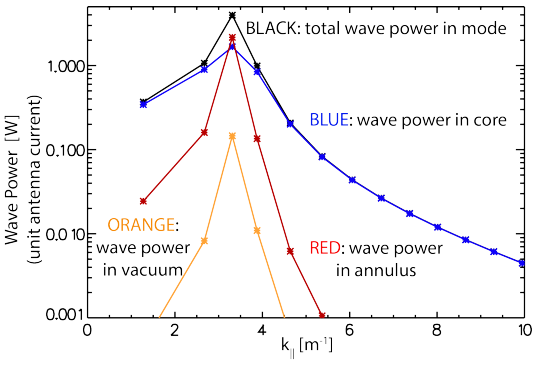

Figure 3: *Wave power conducted in core/annulus/vacuum. $m = 0$ and $n_a = 2\times10^{18}$ m^{-3}.*

We extend the analysis to non-axisymmetric modes in Figure 4a, which plots loading resistance on a linear scale from modes with $m = -3$ to $m = +3$. Modes are weighted by $|c_m|^2$, with c_m the azimuthal Fourier component for an antenna of $\pi/2$ span: $|c_0|^2 = 1/16$ and $|c_m|^2 = \sin^2(m\pi/2)/(\pi m)^2$ for $m \neq 0$. We include the azimuthal spectral weighting but not the axial weighting because the azimuthal weighting is essentially fixed and does not change with the choice of antenna phase. Similar to the $m = 0$ case of Fig. 1, for each m loading resistance peaks for a handful of modes. However, the $k_{||}$ of these peak increase with m. Thus, the condition for maximal loading, one-quarter wavelength fitting in the annulus, holds only very appoximately for $m \neq 0$ (Fig. 4b), and this dependence on m will be the subject of future investigation.

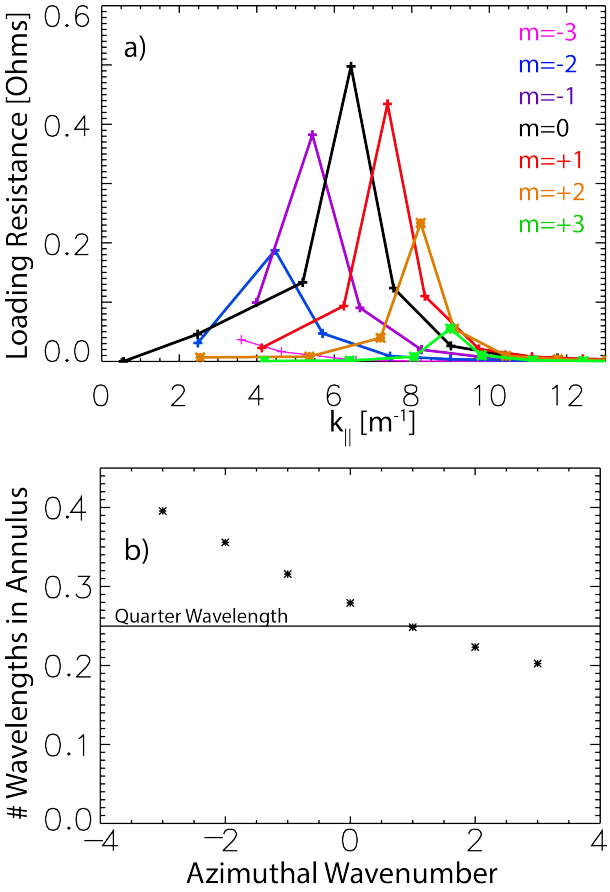

Figure 4: *a) Loading resistance for various m. b) Numer of wavelengths in the annulus for various m.* $n_a = 2 \times 10^{18}$ m^{-3}.

The cylindrical cold-plasma model contains modes that conduct a signficant fraction of power in the lower-density annulus region and that carry a significant fraction of the total power. Such modes are good candidates for explaining the SOL losses in NSTX. A clear next step would be to test if the Poynting flux is field-aligned, as observed in experiments. This requires a rather detailed study, as the Poynting flux will vary both in z and ϕ due to interference of modes. Ultimately, this work is part of an effort to include the proper edge damping into full-wave codes so that they can reproduce the losses observed in NSTX and predict their importance for ITER.

This work was supported by DOE Contract No. DE-AC02-09CH11466.

References

[1] J.C. Hosea *et al.*, Phys. Plasma, **15**, 056104 (2008)

[2] R.J. Perkins *et al.*, Phys. Rev. Lett **109**, 045001 (2012)

[3] N. Bertelli *et al*, Nucl. Fusion **54** 083004 (2014)

[4] N. Bertelli, to appear in AIP Conf. Proc.

[5] J.C. Hosea and R.M. Sinclair, Phys. Rev. Lett. **23** 3 (1969)

PPPL PRINCETON PLASMA PHYSICS LABORATORY

Princeton Plasma Physics Laboratory
Office of Reports and Publications

Managed by
Princeton University

under contract with the
U.S. Department of Energy
(DE-AC02-09CH11466)

P.O. Box 451, Princeton, NJ 08543
Phone: 609-243-2245
Fax: 609-243-2751

E-mail: publications@pppl.gov

Website: http://www.pppl.gov